Reverse Electrodialysis – Multi Effect Distillation Heat Engine Fed by Lithium Chloride Solutions

Francesco Giacalone, Alesandro Tamburini, Andrea Cipollina*, Giorgio Micale

Dipartimento di Ingegneria, Università degli Studi di Palermo, viale delle scienze ed. 6, 90128 Palermo -Italy
andrea.cipollina@unipa.it

Salinity Gradient Heat Engines (SG-HEs) have been proposed as a promising technology for converting low-temperature heat into electricity. The SG-HE includes two different processes: (i) a salinity gradient process where the salinity gradient between two solutions is converted into electricity and (ii) a thermal regeneration process where low-grade heat (T<100°C) is used to re-establish the original salinity gradient of the two streams. Among the proposed working solutions, aqueous solution of lithium chloride has been identified as one of the most promising thanks to its remarkable solubility and activity. In this work, a process model to study the performance of a SG-HE constituted by a Reverse ElectroDialysis (RED) unit coupled with a Multi Effect Distillation (MED) unit fed with lithium chloride solution is presented. The influence of the concentration of the inlet solution in the RED unit and the temperature difference in the evaporators of the MED unit on the performance were evaluated by considering ideal membranes. Furthermore, the impact of membrane permselectivity and resistance on the system performance was evaluated. Results showed promising system efficiencies, making this technology attractive for conversion of low-grade heat (<100°C) into electricity, but membrane properties should be enhanced.

1. Introduction

Waste heat recovery aims to reuse the heat released by industries in their production process in other exploitable energy forms, increasing the energy efficiency of such processes and reducing emissions. It has been estimated that just from the European industrial sector the amount of waste heat released accounts for 300 TWh/year in the 2015 (Papapetrou et al., 2018), with one third of this amount available at temperatures below 200 °C. Any technology able to convert with 10% efficiency such heat will produce an amount of electricity able to cover the energy demand of many countries in Europe such as Denmark, Ireland, or Croatia. A number of technologies have been proposed so far for the recovery of low-grade heat in different forms of energy which are classified in (i) waste heat to heat, (ii) waste heat to cooling and (iii) waste heat to power. In particular, among the waste heat to power processes, salinity gradient heat engines (SG-HEs) appear promising for the conversion of very low temperature heat (<100°C). This innovative heat engine consists of two units:

(i) a power generation unit where a salinity gradient power (SGP) technology exploits the concentration difference between two saline solutions, a concentrate solution (High, H) and a dilute solution (Low, L), to produce electricity; (ii) a thermally driven regeneration unit using low-grade heat to re-establish the original salinity gradient of the two streams. Differently from traditional open-loop SGP applications, where natural salty streams are mixed and then released into the environment, SGP-HEs operate in a closed-loop, where solutions are continuously recirculated from the power unit to the regeneration unit, thus reducing the amount of solutions required, minimizing the fouling potential and overcoming the need for naturally available salinity gradients.

The main salinity gradient technologies proposed so far are (i) reverse electrodialysis (RED) and (ii) pressure retarded osmosis (PRO). In PRO (Tamburini et al., 2016), osmotic membranes are placed in between the two solutions. The chemical potential difference between the solutions generates a water flux from the dilute to the concentrate, which is "retarded" by the application of a hydraulic pressure in the concentrate side,

accumulating pressure energy. In a second step, this pressure energy is converted into electricity in a hydro-turbine. In RED (Giacalone et al., 2018), ionic exchange membranes (IEMs) are alternatively placed between the concentrate solution and the dilute solution, generating repetitive units called "cell pairs". The chemical potential difference between the two solutions and the particular placement of the IEMs generate an ordered flux of ions through the IEMs. This ionic current is converted into electricity in the end-compartments where electrodic reactions occur.

Concerning the regeneration unit, two main strategies have been proposed so far, namely, solvent extraction and salt extraction. In the solvent extraction process, the regeneration of the original concentration of the two streams exiting from the power unit occurs by removing solvent from the exhausted concentrate stream, which is after transferred to the exhausted dilute stream. Then, low grade heat is used to vaporize the solvent from the exhausted concentration stream, like in a thermal desalination process. In this regard, Multi Effects Distillation (MED) and Membrane Distillation (MD) represent the most interesting options. Conversely, in salt extraction strategy, the regeneration of the initial salt concentration is performed by removing the salt from the exhausted dilute solution to dissolve it again into the exhausted concentrated solution. Among the proposed processes, the use of aqueous solutions with thermolytic salts (in particular ammonium bicarbonate) is regarded as the most promising option (Giacalone et al., 2019-a).

This work focused on a reverse electrodialysis heat engine (RED-HE) adopting the solvent extraction strategy. In principle, different solute-solvent couples can be employed in the system. NaCl-water solutions have been the most adopted and studied so far. Hu et al. (2018) and Palenzuela et al. (2019) performed modelling analyses on reverse electrodialysis-multi effect distillation heat engine (RED-MED HE). Results highlighted the interesting performance of such system in the recovery of low-grade heat with efficiency up to 6.6 %. Long et al. (2016) and Micari et al. (2019), proposed modelling analysis of reverse electrodialysis – membrane distillation heat engine (RED-MD HE) unit. Lower efficiencies were found but the system is simpler and is suitable for small-scale applications.

In the last year, new salt-solutions have been proposed in such applications in order to enhance the process performances of the system. Giacalone et al. (2019-b) investigated the theoretical impact of using different salts in ideal RED-HE, evaluating the heat engine efficiencies on the basis of the Gibbs free energy of the mixing and the latent heat required for the regeneration of the solutions. Results highlighted that, among the screened salts, LiCl is one of the most promising thanks to its remarkable solubility and activity.

In this work, an integrated process model was developed in Excel® to study the performance of a Reverse Electrodialysis Multi Effect Distillation heat engine fed with LiCl-water solutions. Firstly, the influence of the solution concentrations fed to the RED unit on the system efficiency is investigated by considering ideal IEMs. Moreover, for the case of the concentrations providing the highest efficiency, the impact of membrane properties (i.e. permselectivity and resistance) on the heat engine efficiency is evaluated.

2. Method

The whole model consists of two main sub-models including (i) the RED model and (ii) the MED model. The two sub-models are linked by means of mass balance in the mixing processes. The integrated model is developed in Excel® using visual basic Macro. A schematic representation of the process is depicted in Fig. 1.
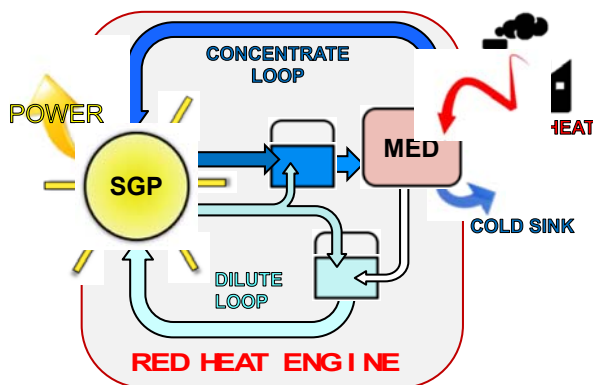

Figure 1: Schematic representation of the RED-MED HE with solvent extraction regeneration unit.

The RED process is modelled considering a mono-dimensional approach, according to those described in previous literature papers (Giacalone et al., 2018, Micari et al., 2019) for the case of NaCl-water solution. Here

the model is further developed by adopting correlations to evaluate the properties of aqueous solution of LiCl as a function of the solution concentration and working temperature. In particular, correlations for solution density, viscosity, conductivity and specific heat capacity are evaluated by fitting experimental results available in the literature (Isono T., 1985, Tanaka,K. et al.; 1991, He et al. 2014). Activity and osmotic coefficients are evaluated according to the Pitzer's Model (Pitzer et al., 1991), adopting virial coefficients computed by fitting literature data (Gibbard et al., 1973).

For given operating conditions (i.e. solution velocities and concentrations), membrane properties (i.e. permselectivity and resistance), stack sizes and configuration (i.e. length, wide, cell pair number, spacer), the model computes the maximum net power output (considering the pumping power required to fed the solutions to the units) and the outlet conditions of the two solutions (flow rate and concentration). Power is always reported in the form of power density (P_d), that is power divided by the total cell pair area.

As shown in Fig. 1, the solutions exiting from the RED unit are partially mixed. This process is required in order to restore the salt content in the concentrate stream, because in the MED process just solvent is recovered and salt has to be transferred in the regeneration in the opposite direction of the RED one (i.e. from the dilute to the concentrate). Thus, part of the dilute, containing the amount of salt transferred within the RED unit, is added to the concentrate. After this step, the resulting solution is fed to the MED where part of the solvent is recovered, restoring the original concentration of the concentrate. Finally, the solvent produced in the MED process is added to the dilute solution exiting from the RED unit, restoring its original concentration.

The MED process is modelled by considering mass and heat balances stage by stage. The modelling approach is analogous to the one used in a previous work (Giacalone et al., 2019), but here the model is further developed in order to consider (i) the distillate produced by the flash phenomena within the MED unit and (ii) the heat required to preheat the inlet solutions. As reported in Ortega-Delgado et al. (2017) and El Dessouky et al. (2002), excluding the first effect, the solution entering in the effect ($w_{sol,k}^{in}$) undergoes a flashing process due to pressure reduction, producing additional vapour ($w_{vap,k}^{F}$):

$$w_{vap,k}^{F} = \frac{w_{sol,k}^{in}\,\overline{c_{p,s}}\left(T_{sol,\,k}^{in,ef} - T_{sol,k}^{F}\right)}{\lambda_{ev,k}} \tag{1}$$

where $\overline{c_{p,s}}$ is the specific heat of the solutions at the average solution temperature, $T_{sol,\,k}^{in,ef}$ is the temperature of the solution entering the k-th effect, $T_{sol,k}^{F}$ is the temperature of the solution after the flashing (evaluated via non-equilibrium allowance (El Dessouky et al., 2002)), $\lambda_{ev,k}$ is the heat of vaporization of the solution at the inlet temperature in the effect.

Similarly, the distillate undergoes a flashing process in the flashing box, resulting in a further thermal recovery. The amount of vapour vaporized in the flashing box ($w_{dist,k}^{F}$) is given by:

$$w_{dist,k}^{F} = \frac{w_{dist_{k-1}}\,\overline{c_{p,d}}\left(T_{vap,k-1}^{cond} - T_{vap,k}^{cond,F}\right)}{\lambda_{ev,k}} \tag{2}$$

where $w_{dist_{k-1}}$ is the distillate mass flow rate coming from the previous flashing box, $\overline{c_{p,d}}$ is the specific heat of water, $T_{vap,k}^{cond,F}$ is the temperature of the distillate exiting from the effect, $T_{vap,k-1}^{cond}$ is the temperature of the distillate coming from the previous flashing box (evaluated via non-equilibrium allowance (El Dessouky et al., 2002)), $\lambda_{ev,k}$ is the heat of vaporization of the distillate.

The preheating of the solution from operating temperature of the RED unit (i.e. 25°C) to the temperature of the first effect is achieved in the preheaters by using a fraction of the vapour produced in the previous effect (β). For a generic preheater:

$$w_{sol}^{in}\,\overline{c_{p,s}}\left(T_{preh,k} - T_{preh,k+1}\right) = \beta\,w_{dist,k}\lambda_{ev,k} + \beta w_{dist,k}\overline{c_{p,v}}(BPE_k) \tag{3}$$

where w_{sol}^{in} is the mass flow rate of the solution entering in MED, $\overline{c_{p,v}}$ is the specific heat of the vapour, $T_{preh,k}$ is the outlet solution temperature of the pre-heater, $T_{preh,k+1}$ is the inlet solution temperature in the pre-heater, BPE_k is the boiling point elevation (BPE) of the vapour produced in the k-th effect.

For a given temperature difference between brine and vapour in the evaporators of the MED system (ΔT_{exch}) and fixing the lowest allowed pressure (or temperature) in the last effect, the model evaluates the maximum suitable number of effects and the corresponding thermal power required to completely restore the two salt-solutions, closing the loop. The MED model takes also into account the pumping power evaluated by considering a horizontal arrangement of the effects and adopting the very same approach reported in

Palenzuela et al. (2019). The temperature of the waste heat ($T_{wasteheat}$) provided in the first effect is set equal to 100°C for all cases while the temperature of the cooling stream is fixed equal to 20°C. The net thermal efficiency of the system (η_{th}) is given by the ratio between the net electrical power produced in the RED unit (i.e. the gross electrical power produced minus the pumping power of the RED and MED processes) and the thermal power required in the MED unit.

Simulations were carried out by considering a RED unit consisting of 500 cell pairs with a membrane area of 0.5x0.5 m^2 and spacers 155 µm thick. Firstly, the effect of the concentrations of the two inlet solutions fed to the RED unit (high-concentration $C_{H,in}$ and low-concentration $C_{L,in}$, respectively) in the range 1 to 14 mol/l and 0.01 to 0.5 mol/l, respectively, was investigated. In order to assess the potential of this heat engine, ideal IEMs were considered: in particular, average permselectivity (α) was assumed as 100 %, water and salt permeability were neglected and resistance (R_{IEMs}) was set to 0.1 Ωcm^2. Concerning the MED unit, ΔT_{exch} was set to 2°C, while the lowest allowed pressure value in the last effect was fixed at 0.05 bar. In the final part of the work, the influence of the average IEMs properties on the performance of the system is studied by varying independently α in the range 50–100 % and R_{IEMs} in the range 0.1 – 7 Ωcm^2.

3. Results and discussion

The first sensitivity analysis, reported in fig. 2, shows the net power density at (P_d) and the specific thermal consumption (STC) of an ideal RED-MED HE system as a function of the RED inlet concentration of the two solutions. Notably, in all simulations, the velocity of the high-concentration and low-concentration solutions fed in the RED unit ($v_{H,in}$ and $v_{L,in}$) are set to 0.5 cm/s, corresponding to feed flowrates of 560 l/h.

The power density generated by the RED unit increases with the salinity gradient difference ($C_{H,in}$-$C_{L,in}$) in all the range under investigation (fig. 2a). P_d is significantly affected by the high solution concentration, while a far less marked variation is encountered when the dilute solution concentration increases. As a matter of fact, due to the high residence time of the solutions in the RED unit (i.e. long channel and low feed velocity) and the low IEMs resistance, the inlet concentration of the solutions within the channel undergoes a large variation along the stack, thus mitigating the impact of the dilute solution concentration. This effect is more evident when high $C_{H,in}$ is considered due to the high driving forces involved which causes large ions fluxes and corresponding higher concentration variation. By using ideal IEMs, power density of 150 W/m^2 could be theoretically reached by using saturated solution of LiCl. As shown in fig. 2b STC increases with the high solution concentration. The higher the solution concentration, the higher the BPE in the evaporators which reduces the available temperature difference between the first and the last effect of the MED unit, thus limiting the total number of effects. An increase of $C_{H,in}$ from 1 to 14 mol/l significantly reduces the number of effects from 24 to 2, increasing the STC from 60-90 kWh/m^3 to 360-380 kWh/m^3.
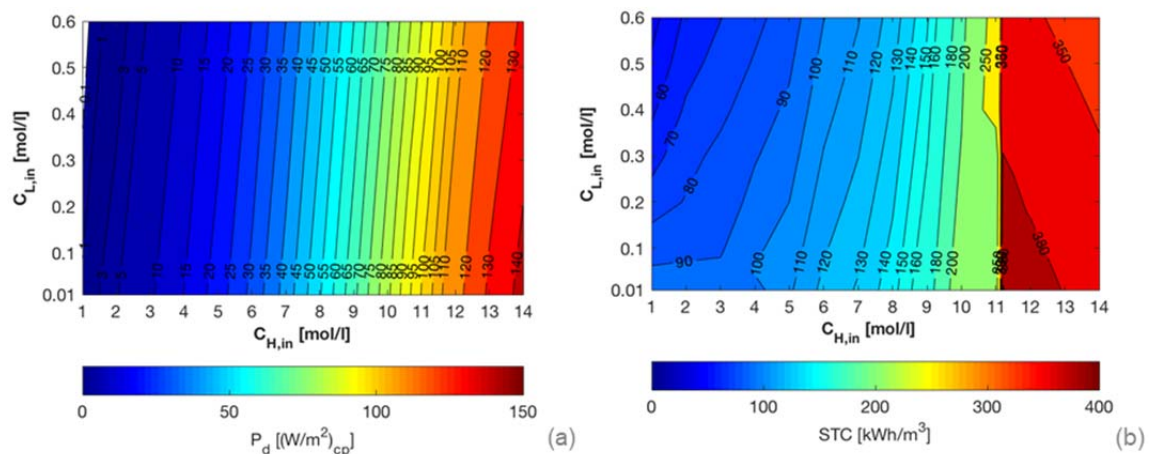

Figure 2: Power density (a) and specific thermal consumption as a function of the concentration of the RED unit feed solutions. RED unit consisting of 500 cell pairs 0.5x0.5 m^2 equipped with ideal IEMs (α=100 % R_{IEMs}=0.1 Ωcm^2), $v_{H,in}$=$v_{L,in}$=0.5 cm/s, ΔT_{exch}=2°C, $T_{waste-heat}$ =100 °C.

The ratio between the net power generated by the RED unit and thermal power consumption of the MED unit gives the thermal efficiency η_{th} of the system. Figure 3 shows η_{th} as a function of the concentration of the solutions for the investigated ideal RED-MED HE. For a fixed dilute inlet concentration and high inlet

concentration from 1 to 7 mol/l, an increase of $C_{H,in}$ results into an increase of η_{th}. For higher inlet concentrations, the behaviour of the efficiency is irregular due to large impact of the BPE on the STC. At concentration higher than 11 mol/l STC grows faster than P_d. The highest thermal efficiency equal to 8.7 % in achieved in the case of C_H=11 mol/l and C_L=0.05 mol/l.
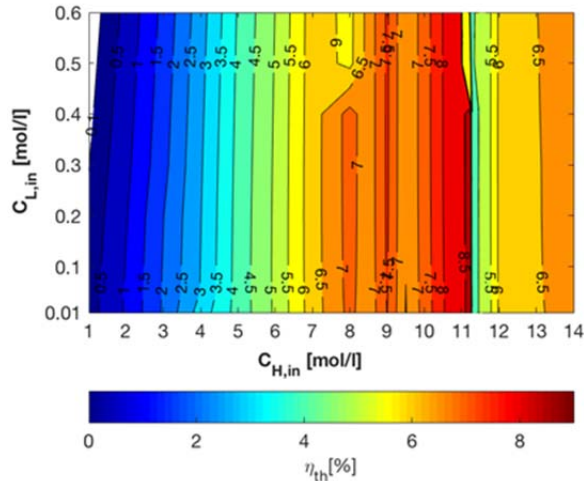

Figure 3: Thermal efficiency as a function of the concentration of the RED unit feed solutions. RED unit consisting of 500 cell pairs 0.5x 0.5 m^2 equipped with ideal IEMs (α=100 % R_{IEMs}=0.1 Ωcm^2), $v_{H,in}$=$v_{L,in}$=0.5 cm/s, ΔT_{exch} =2 °C, $T_{waste\ heat}$ =100 °C.

For the case of these "highly performing concentrations" (C_H=11 mol/l and C_L=0.05 mol/l), the influence of IEMs resistance and permselectivity on the system efficiency was analysed. Both properties significantly affect the performance of the whole RED-HE, due to the large influence on the power density. Figures 4a shows the impact of the IEMs resistance on P_d and η_{th}, at a given value of α (α=100 %), while Figures 4b shows the impact of the permselectivity on the same parameters, at a given value of R_{IEM} (R_{IEM} =0.1 Ωcm^2).

The increase of the resistance from 0.1 to 7 Ωcm^2 considerably reduces P_d from ~100 W/m^2 to ~20 W/m^2, resulting in an efficiency reduction from 8.7 % to 1.2 % (fig. 4a). The sharp drop of efficiency for IEMs resistance shifting from 5 to 6 Ωcm^2 is due to the decrease of the number of effects from 3 to 2.

The decrease of the permselectivity from 100 % to 50 % significantly reduces P_d from ~100 W/m^2 to ~30 W/m^2, leading to an efficiency reduction from 8.7 % to 2.7 % (fig. 4b).
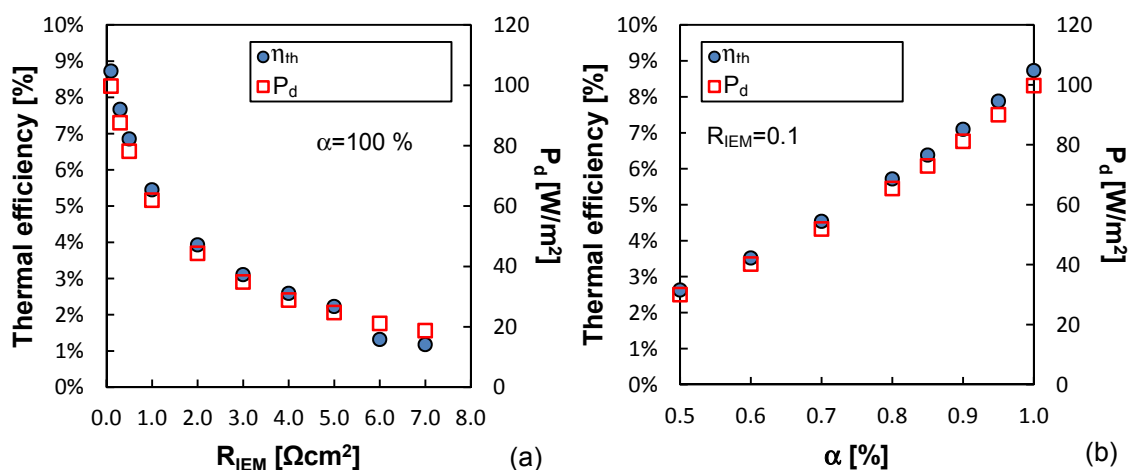

Figure 4: Power density and thermal efficiency as a function of the average IEM resistance fixing the average permselectivity to 100 % (a) and as a function of the average IEM permselectivity fixing the average resistance to 0.1 Ωcm^2 (b). RED unit consisting of 500 cell pairs 0.5x0.5 m^2 fed with LiCl solution $C_{H,in}$=11 mol/l and $C_{L,in}$=0.05 mol/l $v_{H,in}$=$v_{L,in}$=0.5 cm/s, ΔT_{exch}=2 °C, $T_{waste-heat}$=100 °C.

4. Conclusions

In this work, the performance of a RED-MED HE fed with aqueous solutions of LiCl was investigated. The adoption of these solutions in a system equipped with ideal membranes results in high values of efficiency, due to the higher solubility of LiCl compared to the conventional NaCl. In particular, the performance of RED-MED HE equipped with ideal IEMs, results in thermal efficiency up to 8.7 %, making this technology interesting in the field of low-grade waste heat recovery. This value corresponds to ~40 % of the maximum theoretical Carnot efficiency. The performance of current RED HE is significantly affected by the performance of current membranes: significant reductions, with respect to the ideal case, are observed as a result of the resistance and permselectivity values exhibited by the membranes. Thus, future developments of ionic exchange membranes are required in order to approach the promising performance of the ideal membrane - heat engine here investigated.

Acknowledgments

References

El-Dessouky, H.T.; Ettouney, H.M. Fundamentals of Salt Water Desalination, Elsevier, Amsterdam, The Netherlands, 2002.

Giacalone F., Catrini P., Tamburini A., Cipollina A., Piacentino A., Micale G., 2018, Exergy Analysis of Reverse Electrodialysis. Energy Conversion and Management, 164, 588-602.

Giacalone F., Vassallo F., Griffin L., Ferrari M.C., Micale G., Scargiali F., Tamburini A., Cipollina A., 2019-a, Thermolytic reverse electrodialysis heat engine: model development, T integration and performance analysis, Energy Conversion and Management, 189, 1-13.

Giacalone F., Olkis C., Santori G., Cipollina A., Brandani S., Micale G., 2019-b, Novel solutions for closed-loop Reverse Electrodialysis: thermodynamic characterisation and perspective analysis, Energy, 166, 674-689.

Gibbard H.F., Scatchard G., 1973, Liquid-vapor equilibrium of aqueous lithium chloride, from 25 to 100. deg. and from 1.0 to 18.5 molal, and related properties, J Chem Eng Data, 18, 293-298.

He Y., Gao N., Chen G., 2014, Isobaric specific heat capacity of typical lithium chloride liquid desiccants using scanning calorimetry, The Journal of Chemical Thermodynamics, 70, 81-87.

Hu J., Xu S., Wu X., Wu D., Jin D., Wang P., Leng P., 2018, Theoretical simulation and evaluation for the performance of the hybrid multi-effect distillation — reverse electrodialysis power generation system, Desalination, 443, 172–183.

Isono T., 1985, Densities, Viscosities, and Electrolytic Conductivities of Concentrated Aqueous Solutions of 31 Solutes in the Temperature Range 15-55 C and Empirical Equations for the Relative Viscosity, Rikagaku Kenkyusho Hokoku, 61, 53-79.

Long R., Li B., Liu Z., Liu W., 2017, Hybrid membrane distillation-reverse electrodialysis electricity generation system to harvest low-grade thermal energy, J. Memb. Sci. 525, 107–115.

Micari M., Cipollina A., Giacalone F., Kosmadakis G., Papapetrou M., Zaragoza G., Micale G., Tamburini A., 2019, Towards the first proof of the concept of a Reverse ElectroDialysis-Membrane Distillation Heat Engine, Desalination, 453, 77-88.

Ortega-Delgado B., García-Rodríguez L., Alarcón-Padilla D. C., 2017, Opportunities of improvement of the MED seawater desalination process by pretreatments allowing high-temperature operation, Desalin. Water Treat., 97, 94–108.

Palenzuela P., Micari M., Ortega-Delgado B., Giacalone F., Zaragoza G., Alarcón-Padilla D. C., Cipollina A., Tamburini A., Micale G., 2018, Performance Analysis of a RED-MED Salinity Gradient Heat Engine, Energies 11, 3385.

Papapetrou M., Kosmadakis G., Cipollina A., La Commare U., Micale G., 2018, Industrial waste heat: Estimation of the technically available resource in the EU per industrial sector, temperature level and country, Appl. Therm. Eng. 138, 207–216.

Pitzer K. S., 1991, Activity coefficients in electrolyte solutions, CRC Press, London, UK.

Tamburini A., Giacalone F., Cipollina A., Grisafi F., Vella G., Micale G., 2016, Pressure Retarded osmosis: a membrane process for environmental sustainability, Chemical Engineering Transactions, 2016, 47, 355-360.

Tanaka,K.;Tamamushi,R.A, 1991, Physico-chemical Study of Concentrated Aqueous Solutions of Lithium Chloride, Zeitschrift für Naturforschung A, 46, 141-147.